

POD analysis of heat transport in the solar corona from SDO images

Diana Gamborino¹, Diego del-Castillo-Negrete² and Julio J. Martinell¹

¹*Instituto de Ciencias Nucleares, UNAM, A. Postal 70-543, México D.F., Mexico*

²*Oak Ridge National Laboratory, Oak Ridge, TN, USA*

I. Introduction. The solar corona is heated by some mechanism that is still not totally clear but is likely related to upward propagating Alfvén waves carrying energy from the photosphere or to dissipation of magnetic energy by magnetic reconnection. These processes release energy mainly in active regions and then the energy has to propagate to other regions in order to maintain the whole corona at the observed high temperatures. The global heat transport is very much influenced by the complex magnetic field geometry which couples distant regions of the solar corona. This would be expected to produce nonlocal effects in the heat transport leading to non-diffusive processes. Exploring this possibility requires, among other things, a systematic quantitative method to analyze the spatio-temporal evolution of the temperature from observational data. The approach proposed in this paper is based on the use of proper orthogonal decomposition (POD) methods. We analyze images of the solar corona taken by the Solar Dynamics Observatory (SDO) over a period of time following an explosive event focusing on the evolution of a heat pulse. The images are first processed with the SolarSoft package to obtain maps of the Emission Measure and of the temperature over the full solar disk. Then, the region of interest is selected and it is analyzed using two techniques based on POD methods. These are especially well suited for time dependent events.

II. Images and temperature maps.

The event analyzed took place on 31/8/2012 at around 20:00 UT. There were seven active regions on the visible solar disk. Region 1562 was the originator of the solar flare having strength C8.4. Using the combination of six filters for the coronal emission as measured by AIA instrument of SDO, the dual maps for the EM and temperature are obtained, following the techniques developed in [1]. The differential emission measure $DEM = d[EM(T, x, y, z)]/dT = n^2 dh/dT$ is used to describe the temperature distribution of plasma emitting along the line of sight h and is calculated using the intensities $F_\lambda(x, y)$ of six EUV lines from different ionization states of iron (Fe VIII, IX, XII, XIV, XVI, XVIII), covering the coronal range from $0.6MK \leq T \leq 16MK$. AIA records a full set of near-simultaneous images in each temperature filter with a fixed cadence of 12 seconds. The DEM distribution can be reconstructed from the six filter fluxes $[F_\lambda(x, y)]$ (in each pixel), by inverting the equation $F_\lambda(x, y) = \int DEM(x, y, T)R_\lambda dT$, where $R_\lambda(T)$ is the filter response. This process is simplified with the method of multi-Gaussian functions in the case of

six-filter data, which is a forward-fitting technique with parameterized DEM distribution functions [1]. The temperature maps were computed for a time sequence covering 16.4 minutes with a cadence of 12 seconds, as provided by the AIA data. The EM (left) and temperature (right) maps are shown in Figure 1 for a given time, together with a zoom to our region of interest for a sequence of times.

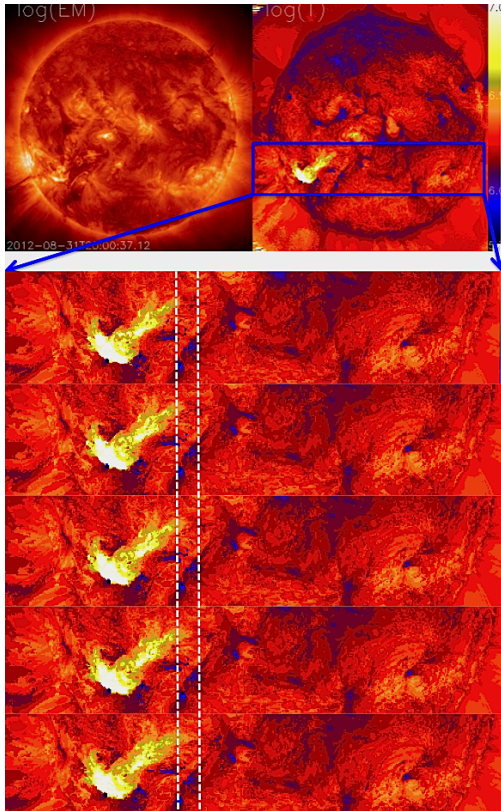


Figure 1: EM and temperature maps with zoom at different times of the region of the heat front.

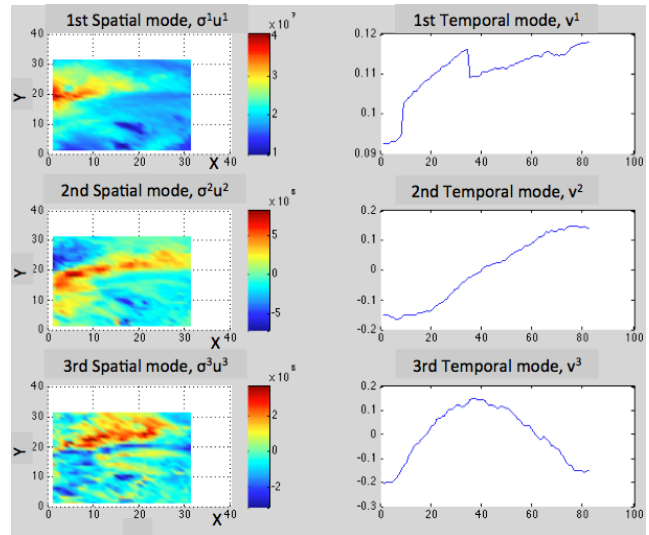


Figure 2: Spatial modes $u_k(r_i)$ (left) and temporal modes $v_k(t_j)$ (right) for $k = 1, 2, 3$ in topos-chronos analysis. Space modes are “refolded” to a 2D map

III. POD methods of analysis.

The Singular Value Decomposition (SVD) is, generally speaking, a mathematical method based on matrix algebra that allows us to build a new basis in which the data is optimally represented. It is a powerful tool because it helps us extract dominant features and coherent structures that might be hidden in the data by identifying and sorting the dimensions along which the data exhibits greater variation. In this, a matrix \mathbf{A} of dimension $m \times n$ is decomposed as

$$\mathbf{A} = \mathbf{U}\Sigma\mathbf{V}^T \quad \text{or} \quad A = \sum_{i=1}^r \sigma_i u_i v_i^T$$

where \mathbf{U} and \mathbf{V} are unitary square matrices and Σ is diagonal of dimension $m \times n$. The second expression is the tensor product of two vectors where $r = \text{rank}(A)$. Here u_i and v_i are the i -th columns of \mathbf{U} and \mathbf{V} respectively. The usefulness of this representation is that if a matrix is to be approximated by another of lower rank k , the Eckart-Young Theorem assures that

$$A_k = \sum_{i=1}^k \sigma_i u_i v_i^T \quad (1)$$

is the optimal (in the L2 norm sense) rank- k approximation of A .

SVD is applied to the matrix of the 2D temperature map in the rectangular grid (x_i, y_j) , where $i = 1, \dots, N_x$ and $j = 1, \dots, N_y$, i.e. $A \rightarrow T(x_i, y_j; t)$. The maps change as a function of time. The maximum number of elements in the SVD expansion (eq. (1)) is, therefore, $k = \min\{N_x, N_y\}$. Two different methods based on SVD are applied to extract specific information.

Topos-Chronos. The first method separates temporal and spatial dependencies of the temperature to reveal the dominant structures that underlie the process [2]. Since the whole data is a 3D array $T_{ijk} = T(x_i, y_j, t_k)$ ($k = 1, \dots, N_t$), it has to be reduced to a 2D matrix by “unfolding” the 2D spatial domain into a 1D vector, i.e. $(x_i, y_j) \rightarrow r_n$ with $n = 1, \dots, N_x \times N_y$. Then, SVD is applied to the space-time 2D matrix $T_{nk} = T(r_n, t_k)$ and the truncation to rank k of the representation is

$$A_{ij}^k = \sum_{m=1}^k \sigma^m u^m(r_i) v^m(t_j). \quad (2)$$

where $1 \leq k \leq N^* \equiv \min\{N_x N_y, N_t\}$. The graphic representation of the topos and chronos modes can be seen in Fig. 2 for different ranks.

Using this, it is possible to make an estimate of the thermal conductivity associated with a diffusive process in the corona. First, the thermal flux entering the region of interest can be calculated using the time derivative of $v^k(t)$. Then, the spatial gradient along the x axis is computed from $u^k(r)$ and used to determine the heat flux from Fourier’s Law ($\vec{q}_T = \kappa \nabla k_B T$) in terms of the *thermal conductivity* (κ). Equating the fluxes, κ can be calculated. In computing \vec{q}_T we have to include the fact that a convective flux \vec{q}_u is also present. Thus, the total flux is $\vec{q}_{Tot} = \vec{q}_u + \vec{q}_T$. From the heat transfer equation and assuming that the heat enters the volume only through the left boundary (the others being negligible), it is possible to show that the flux q_1 from this side is

$$\frac{q_1}{k_B} \Big|_{t_j} = \frac{3}{2} \frac{n_e L}{N^2} \sigma^1 \left[\sum_{i=1}^{N_x N_y} u^1(r_i) \right] \frac{dv^1}{dt} \Big|_{t_j} . \quad (3)$$

including only the lowest mode ($r = 1$, providing an adequate representation), where $N = N_x = N_y$, L is the box size and $n_e = 10^{15} m^{-3}$ the plasma density. This is a function of time but its average value is $\langle q_1 \rangle_t = 2.23 \times 10^3 \text{ J m}^{-2} \text{ s}^{-1}$. On the other hand, the convective flux is determined by the pulse speed which is calculated by following an isocontour of temperature in time

obtaining $\langle u_x \rangle_t = 7.56 \times 10^3 \text{ ms}^{-1}$. For a temperature $T = 2.5 \text{ MK}$, the average convective flux is $\langle q_u \rangle_t = n_e T \langle u_x \rangle = 260 \text{ J m}^{-2} \text{ s}^{-1}$. The corresponding value of $\kappa|_t = (q_1|_t - q_u)/|\nabla k_B T|$ averaged over time is $\langle \kappa \rangle_t = 3.02 \times 10^{28} \text{ m}^{-1} \cdot \text{s}^{-1}$. Compared to the collisional value $\kappa_{col} = 3.2 \frac{nk_B T_e \tau_e}{m_e} = 1.315 \times 10^{28} \text{ m}^{-1} \cdot \text{s}^{-1}$ for parallel transport, it is 2.3 times larger, but of the same order.

GLRAM. The second method, called Generalized Low Rank Approximation of Matrices (GLRAM) [3, 4], iteratively computes the matrices that minimize the error in the approximation of the matrix A_i by a low range decomposition product, as given by $(\min \sum_{i=1}^n \|A_i - LM_i R^T\|_F^2)$. In each iteration the error is reduced achieving a fast convergence. The crucial difference with SVD is the way to represent the data. Here, the unitary orthogonal bases L and R do not change in time and the time information is stored in the matrices of singular values M_i which is not necessarily diagonal. This allows to find precise contour maps of the temperature as function of time from which we can obtain the widening of the heat pulse, which determines the type of heat transport. Fig. 3 shows the evolution of the area between two temperatures, which is a measure of the dispersion due to transport. The time scaling is of the form $A_{12} \sim \sigma^2 \sim t^\gamma$. To exclude advection, only the nose of the front is considered as seen in the upper panel. It is found that the exponent is $\gamma = 0.78 < 1$ indicating that the transport is sub-diffusive.

Acknowledgements. This work was partially supported by Projects DGAPA-UNAM IN109115, IN106911 and CONACyT 152905.

References:

- [1] Aschwanden et al., Solar Phys. **283**, 5 (2011).
- [2] S. Futatani, S. Benkadda, and D. del-Castillo-Negrete, Phys. of Plasmas **16**, 042506 (2009).
- [3] J. Ye, Mach. Learn. **61**, 167 (2005).
- [4] D. del-Castillo-Negrete, S.P. Hirshman, D.A. Spong, and E.F. D'Azevedo, J. Comp. Phys., **222**, 265 (2007).

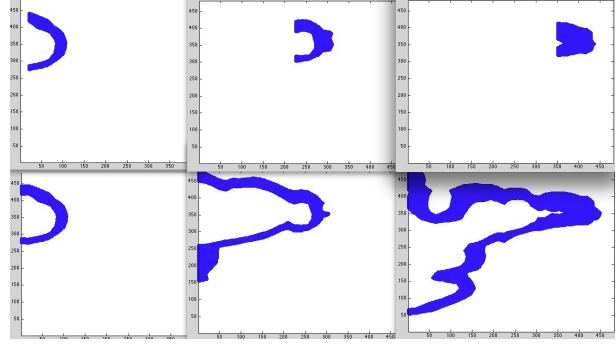


Figure 3: Snapshots of the data interpolation using GLRAM for $n_t = 1, 40, 80$. and for temperature values of 2.5MK. Up: Nose of the thermal pulse. Down: Full structure of thermal pulse.